Two-photon E1M1 decay of $2\,^3P_0$ states in heavy heliumlike ions

I. M. Savukov* and W. R. Johnson†
Department of Physics, 225 Nieuwland Science Hall
University of Notre Dame, Notre Dame, IN 46566
(Dated: April 22, 2019)

Two-photon E1M1 transition rates are evaluated for heliumlike ions with nuclear charges in the range $Z = 50$–94. The two-photon rates modify previously published lifetimes/transition rates of $2\,^3P_0$ states. For isotopes with nuclear spin $I \neq 0$, where hyperfine quenching dominates the $2\,^3P_0$ decay, two-photon contributions are significant; for example, in heliumlike ^{187}Os the two-photon correction is 3% of the total rate. For isotopes with $I = 0$, where the $2\,^3P_0$ decay is unquenched, the E1M1 corrections are even more important reaching 60% for Z=94. Therefore, to aid in the interpretation of experiments on hyperfine quenching in heliumlike ions and to provide a more complete database for unquenched transitions, a knowledge of E1M1 rates is important.

PACS numbers: 31.10.+z, 31.30.Jv, 32.70.Cs, 32.80.-t

I. INTRODUCTION

In recent years, accurate calculations of decay rates of $2\,^3P_0$ states of heliumlike ions have been performed for nuclear charges $Z \leq 94$, with [1, 2] and without [3] consideration of hyperfine quenching. Single photon decay of the $2\,^3P_0$ state to the ground state is strictly forbidden by angular momentum selection rules and only a weak E1 decay to the $2\,^3S_1$ state or an even weaker M1 decay to the $2\,^3P_1$ state is possible for isotopes with nuclear spin $I = 0$. For isotopes with $I \neq 0$, weak transitions induced by the hyperfine interaction also are possible. Until now, corrections to $2\,^3P_0$ decay rates associated with two-photon E1M1 decay have been neglected. For low-Z ions, those corrections are extremely tiny, scaling as Z^{12}; however, for ions such as U^{+90}, the E1M1 decay rate is comparable to the single-photon rate as shown by Drake [4]. Two-photon E1M1 rates are also expected to be significant for heavy two-electron ions other than U^{+90} and calculations are needed. To date, the only ion with $Z > 50$ for which a measurement of hyperfine quenching has been made is heliumlike gadolinium [2]; for the isotope ^{155}Gd, the E1M1 correction to the lifetime is only 0.08%.

We evaluate two-photon E1M1 transition rates for $2\,^3P_0$ states of heliumlike ions with $Z = 50$–94. The E1M1 rate is a smooth function of Z that follows approximately the Z^{12} law predicted by Drake [4]. Revised lifetimes of $2\,^3P_0$ states for isotopes with $I \neq 0$, where hyperfine quenching occurs, are also given. Additionally, we give $^3P_0 \to 1^1S_0$ rates for ions with $Z = 50-94$ having $I = 0$. Although E1M1 transitions are very interesting for relativistic theories, because of the very large negative-energy contributions to the transition amplitudes, direct measurements of E1M1 transitions have not yet been made.

II. THEORY

A. Two-photon E1M1 transition rate

The differential transition probability for the two-photon E1M1 decay, after summation over the photon polarization states and integration over photon angles, takes the form

$$dw_{FI} = \frac{2}{27\pi}\alpha^8 \omega_1^3 \omega_2^3 d\omega_1 \left(\left|M(1,2)\right|^2 + \left|M(2,1)\right|^2\right), \quad (1)$$

where the photon frequencies are related by energy conservation, $\omega_1 + \omega_2 = E_f - E_i$ and the two-photon matrix element $M(1,2)$ is given by,

$$M(1,2) = \sum_n \frac{\langle i\,|E_1(1)|\,n\rangle\,\langle n\,|M_1(2)|\,f\rangle}{E_n + \omega_1 - E_i} + \frac{\langle i\,|M_1(2)|\,n\rangle\,\langle n\,|E_1(1)|\,f\rangle}{E_n + \omega_2 - E_i}. \quad (2)$$

In this equation, i, f, and n designate initial, final, and intermediate states. Permutation of arguments in the matrix element $M(1,2)$ means that ω_1 and ω_2 should be interchanged in the denominators and in the arguments of dipole matrix elements. Compared to the expression for the 2E1 transition rate given in Ref. [5], there is the extra factor $\alpha^2/4$, owing to differences between magnetic and electric dipole matrix elements.

The matrix element $M(1,2)$ is gauge invariant. The difference between the length and velocity forms of the electric-dipole moment in a local potential is $\langle i\,|\Delta E_1(\omega)|\,j\rangle = a(E_i - E_j - \omega)\,\langle i\,|\chi(\omega)|\,j\rangle$, where $\chi(\omega)$ is the gauge operator defined in Ref. [3] and a is a constant of proportionality. Using this relation, the completeness of the basis, and the commutativity of $M_1(\omega_2)$ and $\chi(\omega_1)$, we find that the length-velocity difference is for the first term

$$\frac{\langle i\,|\Delta E_1(\omega_1)|\,n\rangle\,\langle n\,|M_1(\omega_2)|\,f\rangle}{E_i - E_n - \omega_1} = a\,\langle i\,|\chi(\omega_1) M_1(\omega_2)|\,f\rangle$$

---

[*] Electronic address: isavukov@nd.edu; URL: `http://www.nd.edu/~isavukov`
[†] Electronic address: johnson@nd.edu; URL: `http://www.nd.edu/~johnson`

and for the second term

$$\frac{\langle i\,|M_1(\omega_2)|\,n\rangle\,\langle n\,|\Delta E_1(\omega_1)|\,f\rangle}{E_i - E_n - \omega_2} = -a\,\langle i\,|M_1(\omega_2)\chi(\omega_1)|\,f\rangle\,.$$

Adding the two terms, we obtain $\Delta M(1,2) = 0$. The numerical calculations discussed below give precise seven-digit gauge invariance, in harmony with the theoretical prediction.

After summation over magnetic substates, the two-photon matrix element can be further simplified,

$$M(1,2) = \frac{1}{[J_i]}\left|\sum_n \frac{\langle i\,||E_1(\omega_1)||\,n\rangle\,\langle n\,||M_1(\omega_2)||\,f\rangle}{E_i - E_n - \omega_1} + \frac{\langle i\,||M_1(\omega_2)||\,n\rangle\,\langle n\,||E_1(\omega_1)||\,f\rangle}{E_i - E_n - \omega_2}\right|^2 . \quad (3)$$

Here $[J_i] = 2J_i + 1$ is the degeneracy of the initial state. The quantity $M(1,2)$ is expressed in terms of reduced dipole matrix elements, which can be easily calculated. The units of the reduced magnetic-dipole matrix element, which sometimes differ in literature, are specified here by its relation to the transition rate

$$A_{if} = \frac{2.69735\times 10^{13}}{\lambda^3}\frac{S_{M1}}{g_i}\;s^{-1},$$

where $S_{M1} = \left|\langle i\,||M_1(\omega)||\,f\rangle\right|^2$, g_i is degeneracy of the initial state, and λ is wavelength in Å.

We consider two-photon decay of the $^3P_0$ level in the single-configuration approximation, similar to Ref. [4]. The initial state is $|i\rangle = |1s2p_{1/2}\,[0]\,\rangle$, the intermediate states are $|n\rangle = |1sns\,[1]\,\rangle$ $(n \neq 1)$ or $|1snd\,[1]\,\rangle$, and the final state is the ground state $|f\rangle = |1s^2\,[0]\,\rangle$. Substituting these states into (Eq. 3) we arrive at the expression for the two-photon amplitude used in our calculations:

$$\begin{aligned}
M(1,2) \;=& \sum_{n\neq 1} \frac{\langle 1s_{1/2}2p_{1/2}[0]\,||E_1(\omega_1)||1s_{1/2}ns_{1/2}[1]\,\rangle\,\langle 1s_{1/2}ns_{1/2}[1]\,||M_1(\omega_2)||1s^2_{1/2}[0]\,\rangle}{E_i - E_{1sns_{1/2}[1]} - \omega_1}\\
&+ \sum_n \frac{\langle 1s_{1/2}2p_{1/2}[0]\,||E_1(\omega_1)||1s_{1/2}nd_{3/2}[1]\,\rangle\,\langle 1s_{1/2}nd_{3/2}[1]\,||M_1(\omega_2)||1s^2_{1/2}[0]\,\rangle}{E_i - E_{1snd_{3/2}[1]} - \omega_1}\\
&+ \sum_n \frac{\langle 1s_{1/2}2p_{1/2}[0]\,||M_1(\omega_2)||1s_{1/2}np_{1/2}[1]\,\rangle\,\langle 1s_{1/2}np_{1/2}[1]||E_1(\omega_1)||1s^2_{1/2}[0]\,\rangle}{E_i - E_{1snp_{1/2}[1]} - \omega_2}\\
&+ \sum_n \frac{\langle 1s_{1/2}2p_{1/2}[0]\,||M_1(\omega_2)||1s_{1/2}np_{3/2}[1]\,\rangle\,\langle 1s_{1/2}np_{3/2}[1]||E_1(\omega_1)||1s^2_{1/2}[0]\,\rangle}{E_i - E_{1snp_{3/2}[1]} - \omega_2}. \quad (4)
\end{aligned}$$

With the aid of the expressions for the reduced two-electron matrix elements given explicitly in [3, p. 264], we can rewrite (Eq. 4) in terms of single-electron reduced matrix elements, leading to a result in agreement with that given by Drake [4].

B. Line shape

One problem of two-photon expressions is distinguishing between "pure" and cascade two-photon processes. The separation is needed for calculations of a total rate since the cascade process is already included in a single-photon decay rate but the pure two-photon process is not. (Actually, this provides a good definition for a cascade process.) Although for the off-resonance contribution the cascade process is negligible, near the resonance it dominates. In [4], the subtraction of quadratic resonant terms was used to calculate the pure two-photon contribution. Since some details are not clear, we describe in the appendix a subtraction procedure in more detail. We define a cascade process as the quadratic resonant term with a fixed frequency in the numerator (this was not stated in [4] and is important). This definition is reasonable because it gives a Lorentzian profile and after integration over frequencies of the resonant photon the expected single-photon rate, provided one resonant channel dominates as is the case. Subtracting this cascade process from the total two-photon contribution, we can define the pure two-photon spectrum. Near resonance portion of the spectrum becomes closely antisymmetric and upon symmetric integration will contribute insignificantly. Resonant contributions can then be discarded placing grid points far away from resonant regions and the pure two-photon contribution can be trivially evaluated. In the Appendix, we analyze the line shape of the pure two-photon spectrum near the strong resonance (there is also a second, weaker resonance but its contribution is less important).

III. NUMERICAL METHOD

Since we wish to consider highly-charged ions, we base our calculations on the Dirac equation. To treat small correlation effects, of order $1/Z$, we use three starting potentials: Coulomb potential with $Z = Z_{\rm ion}$, Coulomb potential with $Z = Z_{\rm ion} - 1$, and the model potential $V(r) = -Z/r + v_0(1s, r)$, where $v_0(1s, r)$ is the electrostatic potential of a single $1s$ electron. Among the three, the model potential takes into account correlations most completely, in that experimental energy levels are closely reproduced. Therefore, in our final compilation of two-photon rates, the model potential results are used.

To carry out the sum over intermediate states, for each of the three potentials we use a B-spline basis set consisting of 40 positive-energy and 40 negative-energy basis orbitals for each angular momentum state constrained to a cavity of radius $R = 92/Z_{\rm ion}\ a_0$. The completeness of this basis is reflected by precise gauge invariance: for example, in the Coulomb potential $Z = 92$ for heliumlike uranium, the reduced two-photon matrix elements in the length and the velocity forms are $M(1,2)_l = 2.9395608 \times 10^{-6}$ and $M(1,2)_v = 2.9395610 \times 10^{-6}$. Negative energy contributions, which almost for 2E1 transitions are small, are important in the case of E1M1 transitions.

Since four of the terms in Eq. (4) have resonant energy denominators and the two-photon transition rate is extremely sensitive to photon frequencies ($\sim \omega_1^3\omega_2^3$), we replace the approximate lowest-order energies by accurate two-electron energies in these four terms: $E_i \to E(1s^2\,{}^1S_0)$, $E_{1s2s[1]} \to E(1s2s\,{}^3S_1)$, $E_{1s2p_{1/2}[1]} \to E(1s2p\,{}^3P_0)$, and $E_{1s2p_{3/2}[1]} \to E(1s2p\,{}^1P_1)$, where the accurate energies $E(1snl\,{}^{1,3}L_J)$ are taken from Plante [6]. Similar replacements were used by Drake [4] in his calculations of the two-photon rate for $\rm U^{90+}$.

IV. RESULTS

Using the procedure described in previous section, we compute the two-photon transition rates according to the Eq(1) and after subtraction resonances integrate the differential rate to obtain the total two-photon rate. Since the behavior of the rates with Z is very smooth, we performed calculations only for eleven different ions. Table I summarizes our results for total transition rates. The three potentials, discussed above, give results in close agreement, but the model potential for which length-velocity agreement ranges 0.4-1.5% and so does approximately accuracy should be considered the most accurate. (The precise gauge-invariance is achieved when denominators are not modified in all three cases.) For $\rm U^{90+}$our Coulomb Z potential result (5.567×10^9 s^{-1}) agrees well with Drake's [4] (5.60×10^9 s^{-1}) obtained in the same potential. There is also small E2M2 contribution equal to (0.025×10^9 s^{-1}) which was calculated by Drake [4] for $\rm U^{90+}$. We will neglect it in all our calculations.

TABLE I: E1M1 total transition rates for heliumlike ions in the range $Z = 50 - 92$. The rates were calculated using three different potentials: the Coulomb Z, the Coulomb $Z-1$, and a model potential $V = -Z/r + v_0(1s, r)$. In the model potential case, the difference between results obtained in length and velocity forms are also shown as a measure of accuracy of calculations.

Z	Coul Z	Coul Z-1	MP	(L-V)/L
50	2.939[6]	2.798[6]	2.888[6]	1.7%
54	7.476[6]	7.130[6]	7.354[6]	1.3%
58	1.784[7]	1.706[7]	1.758[7]	1.0%
62	4.032[7]	3.862[7]	3.976[7]	0.8%
66	8.686[7]	8.335[7]	8.575[7]	0.7%
70	1.795[8]	1.725[8]	1.774[8]	0.5%
74	3.574[8]	3.442[8]	3.536[8]	0.5%
79	8.090[8]	7.808[8]	8.014[8]	0.5%
82	1.291[9]	1.247[9]	1.279[9]	0.4%
86	2.355[9]	2.280[9]	2.337[9]	0.4%
92	5.567[9]	5.403[9]	5.530[9]	0.5%

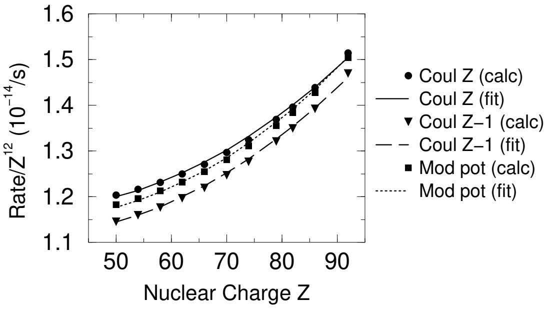

FIG. 1: Polynomial interpolations of Z-dependences for total transition rates calculated in the three starting potentials.

In the table, we provide one extra digit beyond accuracy for better interpolation. For convenience, we also give the interpolation polynomials that fit our calculated rates with sufficient accuracy. In the case of the Coulomb Z potential the polynomial is $Z^{12}(1.28 - 6.4 \times 10^{-3}Z + 9.60 \times 10^{-5}Z^2)$; in the case of the Coulomb $Z-1$ potential the polynomial is $Z^{12}(1.22 - 6.4 \times 10^{-3}Z + 9.8 \times 10^{-5}Z^2)$; and in the case of the model potential the polynomial is $Z^{12}(1.29 - 7.73 \times 10^{-3}Z + 1.10 \times 10^{-4}Z^2)$. The rates in all three cases as well as the fitting polynomials are shown in Fig. 1.

The upper curve corresponds to the Coulomb Z potential, the lower curve to the Coulomb $Z-1$ potential, and the middle one to the model potential. In addition to total rates we also show in (Fig. 2) the frequency distribution of the differential two-photon transition rate for $Z = 92$, $Z = 79$, $Z = 62$, and $Z = 50$. In the case of uranium, $Z = 92$, the shape resembles very closely the distribution given by Drake [4]. The continuous evolution with Z can be seen: the maximum at the center monotonously decreases with Z, but the wings are rapidly developing for lower Z ions.

In the case of $Z = 50$, the wings are large; therefore we

TABLE II: E1M1 two-photon corrections to lifetimes τ (ps) and E1M1 rates A_{E1M1} (1/ns) for ions with hyperfine induced decays.

Ion	Z	τ_{old}	τ_{new}	A_{E1M1}	% change
^{155}Gd	64	13.57	13.56	0.059	0.08%
^{169}Tm	69	8.487	8.476	0.149	0.13%
^{171}Yb	70	1.917	1.916	0.178	0.03%
^{173}Yb	70	2.113	2.112	0.178	0.04%
^{177}Hf	72	1.603	1.602	0.253	0.04%
^{179}Hf	72	2.556	2.554	0.253	0.06%
^{183}W	74	25.54	25.31	0.355	0.91%
^{187}Os	76	59.83	58.11	0.496	2.97%
^{189}Os	76	1.546	1.545	0.496	0.08%
^{191}Ir	77	25.07	24.71	0.584	1.46%
^{193}Ir	77	21.70	21.43	0.584	1.27%
^{195}Pt	78	0.9433	0.9430	0.686	0.06%
^{197}Au	79	23.04	22.62	0.805	1.86%
^{199}Hg	80	1.248	1.247	0.943	0.12%
^{201}Hg	80	1.782	1.779	0.943	0.17%
^{203}Tl	81	0.1215	0.1210	1.10	0.01%
^{205}Tl	81	0.1192	0.1190	1.10	0.01%
^{207}Pb	82	0.8357	0.8350	1.29	0.11%
^{209}Bi	83	0.0041	0.0040	1.50	0.00%
^{223}Ra	88	5.079	4.999	3.14	1.60%
^{229}Th	90	1.955	1.939	4.18	0.82%
^{235}U	92	2.623	2.585	5.54	1.45%
^{239}Pu	94	3.707	3.610	7.29	2.70%

studied the line shape more carefully with a refined scale. The discussion of the behavior near the origin, where resonances are located, is given in the Appendix. From this discussion follows that the integrated contribution from that region is not much different from that of any other part of the spectrum. Since we discovered that E1M1 corrections are significant for ions in the range Z=50-94, we also correct previously calculated values of lifetimes and transition rates for those ions. Tables II and III show previously calculated and corrected rates. Table II gives revised lifetimes for isotopes that have hyperfine induced transitions. We show only the cases where modification changes quoted digits. Table III shows transition rates without hyperfine mixing, when corrections owing to E1-M1 transitions are particularly large.

The difference reaches 57.5% for $Z = 94$. (Drake's prediction in uranium [4] was 46%.) Depending on experimental situation, any ion shown in the table can be potentially used for the measuring E1M1 transition rate.

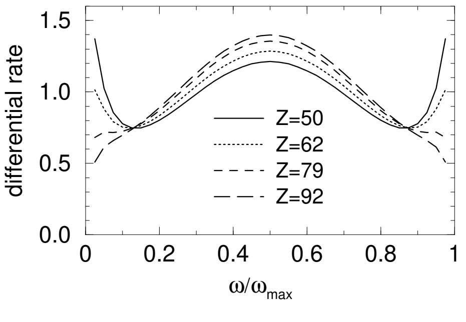

FIG. 2: Differential rate for two-photon decay

TABLE III: E1M1 two-photon corrections to transition rates A (1/s) for ions without hyperfine induced decays.

Z	A_{old}	A_{E1M1}	A_{new}	% change
50	1.363[9]	2.87[6]	1.366[9]	0.21%
51	1.439[9]	3.66[6]	1.443[9]	0.25%
52	1.519[9]	4.63[6]	1.524[9]	0.30%
53	1.605[9]	5.84[6]	1.611[9]	0.36%
54	1.695[9]	7.33[6]	1.702[9]	0.43%
55	1.790[9]	9.16[6]	1.799[9]	0.51%
56	1.891[9]	1.14[7]	1.902[9]	0.60%
57	1.997[9]	1.42[7]	2.011[9]	0.71%
59	2.228[9]	2.16[7]	2.250[9]	0.97%
60	2.353[9]	2.66[7]	2.380[9]	1.13%
62	2.623[9]	3.97[7]	2.663[9]	1.51%
63	2.768[9]	4.84[7]	2.816[9]	1.75%
64	2.925[9]	5.87[7]	2.984[9]	2.01%
65	3.090[9]	7.11[7]	3.161[9]	2.30%
66	3.263[9]	8.59[7]	3.349[9]	2.63%
67	3.446[9]	1.03[8]	3.549[9]	3.00%
68	3.638[9]	1.24[8]	3.762[9]	3.41%
69	3.839[9]	1.49[8]	3.988[9]	3.88%
70	4.049[9]	1.78[8]	4.227[9]	4.39%
71	4.273[9]	2.12[8]	4.485[9]	4.97%
72	4.507[9]	2.53[8]	4.760[9]	5.60%
73	4.754[9]	3.00[8]	5.054[9]	6.31%
74	5.011[9]	3.55[8]	5.366[9]	7.09%
75	5.287[9]	4.20[8]	5.707[9]	7.95%
76	5.574[9]	4.96[8]	6.070[9]	8.89%
77	5.875[9]	5.84[8]	6.459[9]	9.94%
78	6.187[9]	6.86[8]	6.873[9]	11.09%
79	6.315[9]	8.05[8]	7.120[9]	12.75%
80	6.852[9]	9.43[8]	7.795[9]	13.76%
81	7.215[9]	1.10[9]	8.318[9]	15.28%
82	7.663[9]	1.29[9]	8.950[9]	16.79%
83	7.971[9]	1.50[9]	9.470[9]	18.81%
88	1.004[10]	3.14[9]	1.318[10]	31.31%
90	1.093[10]	4.18[9]	1.511[10]	38.28%
92	1.181[10]	5.54[9]	1.735[10]	46.87%
94	1.267[10]	7.29[9]	1.996[10]	57.51%

V. CONCLUSIONS

In this paper, we have calculated E1M1 transition rates for heliumlike ions ($Z = 50 - 94$). The previous lifetime values are improved with adding E1M1 contributions. The large E1M1 corrections in heavy ions can be tested in future experiments and the E1M1 transition rates can be extracted from experiments to study those essentially relativistic transitions.

Acknowledgments

The authors thank R. Marrus for suggesting this problem and acknowledge helpful discussions with Professor L. M. Labzowsky. This work was supported in part by National Science Foundation Grant No. PHY-01-39928.

APPENDIX: ANALYSIS OF THE LINE SHAPE

The two-photon transition matrix element $M(1,2)$ has two poles: one occurs for $n = 2$ in the first term of Eq. (4), when ω_1 equals the $2\,^3P_0 \to 2\,^3S_1$ (E_1) transition energy, and the second occurs for $n = 2$ in the third term term, when ω_1 equals the $2\,^3P_0 \to 2\,^3P_1$ (M_1) transition energy. To obtain the correct line shape, the denominators in each of these pole terms should be modified to include widths of the levels: $E_n \to E_n - i\Gamma/2$. (If the small width of the initial state is neglected, then $\Gamma = \Gamma_n$, the width of the nth level only). The insertion of the imaginary term leads to an almost Lorentzian profile near the resonance. By subtracting the Lorentzians corresponding to the cascade processes or simply single-photon decays, we obtain the purely two-photon decay rate and its spectral distribution. After subtraction, the remaining contribution to the two-photon rate near the resonance region becomes very small when the resonant intermediate level is very narrow, as is the case for the intermediate $2\,^3S_1$ level and the resonances can be ignored in the total two-photon rate. To check that resonant contributions are small, we made fine grid in the resonant region and calculated the resonance contributions. The cascade contribution is large and is calculated separately, using more precise methods. A precise rate for the $2\,^3P_0 \to 2\,^3S_1$ (E_1) transition is given in Ref. [3]. For comparison with experiment, our two-photon line shape should be added to the Lorentzian obtained using the accurate line width and the single-photon transition rate. In this paper, we will show only pure two-photon profile, *i.e.,* what remains after resonances are subtracted.

The analysis of the relative contribution to the two-photon rate from the resonant region, using limit that the width is very small, gives the following expression:

$$I(\omega) \simeq \frac{I_1(\omega_1)}{3\omega_1}\left[\frac{3}{2}\ln|\omega - 1| + \omega + \frac{1}{4}\omega^2\right].$$

In this formula the unit of frequency is chosen the resonant frequency ω_{res}, $I(\omega)$ is the contribution obtained by integration from zero to ω, $I_1(\omega_1)$ is the contribution with the symmetric integration from $-\omega_1$ to $+\omega_1$ with $\omega_1 < 1$. The integrals $I_1(\omega_1)$ and $I(\omega)$ are defined below, and the expansion over small parameter Γ have been carried out:

$$I_1(\omega_1) = A\int\limits_{1-\omega_1}^{1+\omega_1} \frac{x^3 - 1}{(x-1)^2 + \left(\frac{\Gamma}{2}\right)^2}dx \simeq A3\omega_1\Gamma$$

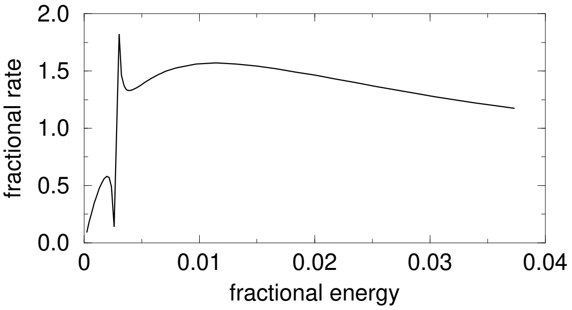

FIG. 3: Near-resonant portion of pure two-photon spectrum

$$\begin{aligned} I(\omega) &= A\int\limits_0^{\omega} \frac{x^3 - 1}{(x-1)^2 + \left(\frac{\Gamma}{2}\right)^2}dx \\ &\simeq A\frac{\Gamma}{2}\left[\frac{3}{2}\ln|\omega - 1| + \omega + \frac{1}{4}\omega^2\right]. \quad \text{(A.1)} \end{aligned}$$

The illustration of the shape of the near resonance differential rate is given in Fig. 3. Here the case $Z = 50$ is considered. The differential rate near the resonance is very large, of order 10^4, and is not shown here. However, owing to a precise cancellation, the total contribution after integration is quite small.

The symmetric integral in the near resonance region owing to very precise cancellation provides better numerical accuracy than asymmetric, but far away from the resonance when $\omega_1 > 1$, instead of the symmetric integral the asymmetric integral has to be used. We assume that only one strong resonance near zero where two-photon differential rate is proportional to ω^3 is present. The integral $I_1(\omega_1)$ is proportional to the frequency ω_1 and to the width of the resonance, and the smaller the width the smaller resonant contribution $I(\omega)$ will be. Using the above equations, it can be shown that the residual resonant contribution to the two-photon rate is insignificant compared to the smooth continuum contribution.

The shape in the near resonance region can be described approximately by the following equation

$$f(x) \approx \frac{1 + x + x^2}{(x-1)} + background$$

if $(x - 1) \gg \Gamma$. The background is the smooth continuum contribution owing to all terms except the resonant term. There is maximum at $x = 0.012$ owing to two-photon continuum for small x behaving like $x^k(1-x)^3$. Depending on the position of most contributing levels, $k = 1 \div 3$. We show the case $Z = 50$ for which the wings are the most pronounced. At the very origin, the differential rate rapidly grows x^3 if x is much less than the any denominator of the terms with large contributions.

The sharp left edge of the wings is owing to the sharp ω^3 dependence of the differential rate near the origin. The located very close to the origin subtracted resonances, which have asymmetric shapes and narrow widths, are shown in Fig. 3 since their differential rate near the resonance frequency is very high and needs different scale. But resonant contributions also decrease so fast that they have no effect on the shown region as well on the total rate.

[1] W. R. Johnson, K. T. Cheng, and D. R. Plante, Phys. Rev. A **55**, 2728 (1997).

[2] P. Indelicato, B. B. Birkett, J.-P. Briand, P. Charles, D. D. Dietrich, R. Marrus, and A. Simionovici, Phys. Rev. Lett. **68**, 1307 (1992).

[3] W. R. Johnson, D. R. Plante, and J. Sapirstein, in Advances in Atomic, Molecular, and Optical Physics, edited by B. Bederson and H. Walther (Addison-Wesley, New York, 1995) **35**, 255 (1995).

[4] G. W. F. Drake, Nuclear Instruments and Methods in Physics Research **B9**, 465 (1985).

[5] A. Derevianko and W. R. Johnson, Phys. Rev. A **56**, 1288 (1997).

[6] D. R. Plante, Ph.D. thesis, University of Notre Dame (1995).